Quantitative assessment of hydrogen diffusion by activated hopping and quantum tunneling in ordered intermetallics

Bhawna Bhatia[1] and David S. Sholl[1,2,*]
[1]*Department of Chemical Engineering, Carnegie Mellon University, Pittsburgh, Pennsylvania 15213, USA*
[2]*National Energy Technology Laboratory, Pittsburgh, Pennsylvania 15236, USA*
(Received 16 May 2005; revised manuscript received 14 July 2005; published 8 December 2005)

Diffusion of hydrogen in metals is a fundamental process in hydrogen storage in metal hydrides, hydrogen purification by metal membranes, and in hydrogen embrittlement. Quantitative applications of existing models for hydrogen diffusion by activated hopping and quantum tunneling require large scale first principles calculations that are not well suited to metal alloys containing many structurally distinct interstitial sites. We applied a semiclassically corrected version of harmonic transition state theory in conjunction with plane wave density functional theory to examine hydrogen diffusion in multiple C15 Laves phase AB_2 compounds and in bcc CuPd. Comparison with experimental data shows that this theory correctly captures the characteristics of hydrogen diffusion in these materials over a wide range of temperatures. This method is well suited to application in complex alloys.

DOI: 10.1103/PhysRevB.72.224302 PACS number(s): 66.30.−h, 61.66.Dk, 71.15.Mb, 82.20.Db

I. INTRODUCTION

The rate at which hydrogen atoms diffuse amongst interstitial sites in metals is of vital importance in several technological areas. H diffusion, in tandem with solubility, controls the throughput of metal membranes for H_2 purification.[1] The rate at which H_2 can be reversibly charged and discharged from metal hydrides is a crucial factor in the applicability of these materials for H_2 storage.[2,3] H diffusion can also be a contributing factor in hydrogen embrittlement of metals.[4]

The fundamental theory of H diffusion in metals has been studied for decades.[5–7] Several different mechanisms for H motion between adjacent interstitial sites have been identified. In many instances, H hopping is an activated process as H atoms must overcome energy barriers between interstitial sites. Transition state theory (TST) provides a useful way to characterize hopping rates in this scenario. Quantum mechanical tunneling can also provide an important contribution to net hopping rates at some temperatures.[5–7]

Several studies have demonstrated methods for accurately predicting the rates of activated hopping and quantum tunneling for H in metals and on metal surfaces by using first principles density functional theory (DFT) to compute the potential energy surface for H.[8–10] Unfortunately, these methods require extensive DFT calculations to characterize a single pair of adjacent sites. For example, Sundell and Wahnström used DFT to compute the three-dimensional potential energy surface of H on Cu(100) with metal atoms held rigid in their relaxed positions and solved the Schrödinger equation numerically to obtain the vibrational states of H in this environment.[9] The same authors estimated the nonadiabatic response of conduction electrons to H motion using DFT data to relate local electronic charge densities to phase shifts. By combining the information from these calculations within a linear coupling model, a detailed description that includes coupling with lattice phonons and the nonadiabatic response of conduction electrons to H motion is possible.[9] Sundell and Wahnström have also recently applied these methods to the hopping of interstitial H in bulk Nb and Ta.[8]

The methods introduced by Sundell and Wahnström provide a comprehensive description of the various contributions to tunneling between adjacent sites for H on metal surfaces or in interstitial sites in bulk materials.[8,9] Application of these methods requires a large number of DFT calculations to be performed for each pair of sites of interest. This limits the application of these methods to complex alloys where large numbers of distinct hopping transition rates must be predicted in order to characterize long-range diffusion.[1,11–13] We have investigated how DFT calculations can be used to rapidly assess the contributions of activated hopping and tunneling in a form that is suitable for examining large numbers of distinct sites. Underlying these calculations is the concept that once the key processes of interest in a particular material are identified, the highly accurate but computationally demanding methods mentioned above could be applied to these processes if necessary.

In Sec. II we describe how semiclassically corrected harmonic transition state theory can be applied to hydrogen hops between interstitial sites in metals using plane wave DFT calculations. In Sec. III we apply this method to hydrogen diffusion in a number of C15 Laves phase intermetallics. Section IV applies the method to H diffusion in bcc CuPd. Our results are summarized and ideas for future extensions of these methods are examined in Sec. V.

II. METHODS

The aim of our calculations is to predict the hopping rate of H between adjacent interstitial sites in a metal alloy. Our approach is to apply semiclassically corrected harmonic transition state theory (SC-HTST) as formulated by Fermann and Auerbach.[14] A crucial feature of this theory is that it requires only the energies and vibrational frequencies of atoms for the energy minima and transition state (TS) associated with a diffusion event, not the full potential energy surface. We ex-

plicitly assume that localized H vibrations are decoupled from vibrations of metal atoms, so the vibrational frequencies of H can be efficiently computed with the positions of all metal atoms constrained. An energy minima then has three vibrational frequencies, ν_i $(i=1,2,3)$, while a TS has two real frequencies, ν_j^{TS} $(j=1,2)$, and one imaginary frequency, $i\nu_{\pm}$.

Within the Fermann and Auerbach approach, the hopping rate across a single transition state at temperature T is written as[14] $k^{SC\text{-}HTST}(T)=k^{HTST}(T)\Gamma(T)$, where $k^{HTST}(T)$ is the harmonic TST hopping rate and $\Gamma(T)$ is the tunneling correction. The HTST hopping rate is $k^{HTST}(T)=\nu^{HTST}(T)\exp(-E_a/kT)$ where E_a is the classical energy difference between the minimum and TS, k is Boltzmann's constant, and

$$\nu^{HTST}(T)=\left[\prod_{i=1}^{3}\nu_i f(h\nu_i/2kT)\right]\Bigg/\left[\prod_{j=1}^{2}\nu_j^{TS} f(h\nu_j^{TS}/2kT)\right]. \quad (1)$$

Here, h is Planck's constant and $f(x)=\sinh(x)/x$. This version of HTST includes the quantization of H vibration, so it accounts for zero-point energy corrections to the classical activation energy, E_a. At low temperatures, the net HTST activation energy becomes $E_{ZP}=E_a-\Sigma_i h\nu_i/2+\Sigma_j h\nu_j^{TS}/2$. In describing the tunneling correction to the net hopping rate, it is convenient to define $\theta_0=(\pi E_{ZP})/(h\nu_{\pm})$. The semiclassical correction is then[14]

$$\Gamma(T)=\frac{\exp(E_{ZP}/kT)}{1+\exp(2\theta_0)}+\frac{1}{2}\int_{-\infty}^{\theta_0}d\theta\,\mathrm{sech}^2\theta\exp\left(\frac{h\nu_{\pm}\theta}{\pi kT}\right). \quad (2)$$

This integral is well behaved and straightforward to evaluate numerically. A detailed discussion of the derivation of this semiclassical correction and its relationship to more detailed multidimensional approaches has been given by Fermann and Auerbach.[14] This method arises from a formulation of quantum rate theory that includes contributions from all energetically allowed reactant and product states.

A key approximation in the SC-HTST description above is that no explicit coupling between the mobile atom and environmental degrees of freedom such as lattice phonons or conduction electrons is included. These effects can renormalize the hopping rate at sufficiently low temperatures.[9] To include these effects on any particular site-to-site hop of interest, a more detailed treatment such as the one performed by Sundell and Wahnström[9] would be necessary.

It is also important to note that the relatively simple form of Eq. (2) is only possible because of the approximation that the potential energy surface describing both the transition state and energy minima is harmonic. Anharmonic corrections to the vibrational energy levels of interstitial H can be determined if DFT calculations are used to calculate a detailed potential energy surface, and it would be possible to include this information within the TST portion of the theory described above. The results of Fermann and Auerbach are based on earlier work by Hernandez and Miller[15] that included anharmonic corrections to the harmonic potential energy surface. This earlier work may offer one fruitful direction for extending Eq. (2) to include anharmonicity in the potential energy surface of interstitial H.

Plane wave DFT calculations have provided a useful computational tool for making quantitative predictions regarding the binding and diffusion of H in interstitial sites in pure metals,[16] disordered alloys,[17] as well as on metal surfaces.[18,19] DFT has also been used by Hong and Fu[20] to examine H binding in e and g sites of a series of C15 ZrX_2 materials. We have performed plane wave DFT calculations to examine H diffusion in ZrX_2 where X=V, Cr, Mn, Fe, and Co and $HfTi_2$, using the Vienna *ab initio* Simulation Package (VASP)[21] using the PW91-GGA exchange-correlation functional. As noted by Hong and Fu, $ZrMn_2$ in reality adopts a hexagonal C14 structure.[20] All calculations for this material below are for the hypothetical C15 structure.[20] Spin polarization was used for $ZrMn_2$, $ZrFe_2$, and $ZrCo_2$. A computational cell extended by periodic boundary conditions was used to describe a material of infinite extent. A cubic computational cell of A_8B_{16} in the C15 structure was used for all calculations. k-space was sampled using $3\times3\times3$ k points positioned using the Monkhorst-Pack scheme. Results using larger numbers of k points gave only very minor total energy differences from calculations with $3\times3\times3$ k points. A cutoff energy of 270 eV was used throughout. Geometries were optimized until the forces on all unconstrained atoms were less than 0.03 eV/Å. Unless otherwise specified, all atoms were allowed to relax during geometry optimizations.

For interstitial H in ZrX_2 (X=V, Cr, Mn, Fe, and Co), we first optimized the C15 lattice constant in the absence of H. This gave lattice constants of 7.32, 7.12, 7.06, and 6.90 Å for ZrV_2, $ZrCr_2$, $ZrFe_2$, and $ZrCo_2$, respectively. These compare well with the experimentally established lattice constants of 7.45, 7.21, 7.07, and 6.95 Å.[20,22–25] The DFT-optimized lattice constant for $ZrMn_2$ in the C15 structure is 7.00 Å. All calculations for interstitial H in these materials were performed by placing a single H atom in the computational supercell, corresponding to a net stoichiometry of $AB_2H_{0.125}$. A slightly different procedure was necessary to examine interstitial H in $HfTi_2$, since it has been established both experimentally[26] and in our prior DFT calculations[27] that the C15 crystal structure for this material is only stable in the presence of quite high concentrations of interstitial H. We began by optimizing the lattice constant for $HfTi_2H_4$ with each H atom occupying an e site in the C15 crystal structure. This calculation yields a lattice constant of 8.1 Å, which can be compared to the experimental value of 8.09 Å.[28] Calculations examining H mobility in this material were performed using a supercell comprised of $Hf_8Ti_{16}H_{32}$ by allowing one H atom to move as described previously.[27]

Transition states for hopping of H between adjacent interstitial sites were determined using the nudged elastic band (NEB) method.[29] All atoms were allowed to relax during these calculations. Following convergence of the NEB calculations, the configuration most closely approximating a transition state was geometry optimized using a quasi-Newton algorithm that converges to critical points on the potential energy surface for starting points sufficiently close to a critical point. This procedure allowed the precise location of the transition states.

TABLE I. A summary of the calculated energy differences between e and g sites in the four ZrX_2 materials examined that experimentally have the C15 structure. A positive value of $\Delta E_{e\to g}$ indicates that the e site is more stable. DFT results are presented from calculations with the experimentally observed lattice constant and with the lattice constant optimized using the indicated DFT functional. The energy differences reported by Hong and Fu from LDA-DFT calculations using the experimentally observed lattice constants (Ref. 20) are also listed. All energies are in eV.

Material	Lattice constant (Å)	$\Delta E_{e\to g}$ GGA-DFT	Lattice constant (Å)	$\Delta E_{e\to g}$ LDA-DFT	$\Delta E_{e\to g}$ Hong and Fu
$ZrFe_2$	7.07 (expt.)	−0.10	7.07 (expt.)	−0.02	+0.006
	7.06 (GGA)	−0.10	6.82 (LDA)	+0.01	-
$ZrCo_2$	6.95 (expt.)	0.06	6.95 (expt.)	0.12	0.074
	6.9 (GGA)	0.06	6.75 (LDA)	0.11	-
ZrV_2	7.45 (expt.)	−0.09	7.45 (expt.)	−0.11	−0.082
	7.32 (GGA)	−0.09	7.15 (LDA)	−0.1	-
$ZrCr_2$	7.21 (expt.)	−0.07	7.21 (expt.)	−0.03	−0.074
	7.1 (GGA)	−0.07	6.97 (LDA)	−0.07	-

Vibrational frequencies for H in local minima and at transition states were calculated by assuming these frequencies are decoupled from metal atom vibrations. With this approximation, the metal atoms were constrained in the geometry associated with the minimum or transition state of interest and the Hessian matrix for local motion of the H atom was estimated using finite difference methods.[17,18,30] This resulted in three real frequencies at each local minimum and two real frequencies at each transition state. Greeley and Mavrikakis recently examined the validity of the decoupling approximation above for H vibration on a Ni surface by computing the vibrational frequencies of H, including the motion of the three nearest surface metal atoms.[18] They found that including these local metal degrees of freedom only changed the vibrational frequencies of H on the surface by $\sim 10\ \mathrm{cm}^{-1}$.

III. H DIFFUSION IN C15 LAVES PHASE AB_2 INTERMETALLICS

We have applied the method described above to a series of C15 Laves phase intermetallics. These materials are ordered alloys with composition AB_2 that have been the subject of extensive experimental studies of H transport.[26,28,31–36] Specifically, we examined $HfTi_2$, $ZrCr_2, ZrFe_2, ZrMn_2, ZrCo_2$, and ZrV_2, each in the C15 structure. We performed plane wave DFT calculations of interstitial hydrogen at low concentration using $A_8B_{16}H$, as discussed in Sec. II. C15 AB_2 materials exhibit three distinct types of tetrahedral sites with local stoichiometry AB_3 (e sites), A_2B_2 (g sites), and B_4 (d sites).[26] Our calculations show that in each material H occupation of d sites is very unfavorable; these sites typically lie $\sim 0.3-1$ eV higher in energy than the preferred e or g site. On this basis, occupation of or hopping involving d sites was excluded from further attention.

Our calculations predict the e site to be the favored site in $HfTi_2$, consistent with neutron scattering experiments.[35,37,38] Our generalized gradient approximation (GGA) calculations predict that g sites are favored in C15 $ZrV_2, ZrCr_2, ZrMn_2$, and $ZrFe_2$ while e sites are energetically preferred in $ZrCo_2$. For the four ZrX_2 materials that exist experimentally in the C15 structure, we have examined these site preferences using GGA-DFT with both the DFT-optimized and experimentally observed lattice constants. The results of these calculations are listed in Table I. It can be seen that the small differences that exist between the DFT-optimized and experimental lattice constants make no appreciable difference in the energy differences between e and g sites. To compare our calculations with the local-density approximation (LDA)-DFT calculations of Hong and Fu,[20] we performed a similar set of calculations for the LDA-optimized lattice constants and experimentally observed lattice constants. These results are also listed in Table I. Because the difference between experimental and DFT-optimized lattice constants are larger for LDA than for GGA, there is more variation in the calculated site energies between the two lattice constants for LDA than for GGA. LDA predicts that the e and g sites in $ZrCo_2$ are close to being isoenergetic. Our LDA calculations predict the same site stabilities as Hong and Fu, although our numerical results for the site energy differences differ by ±0.04 eV from their reported values. It is possible that these differences in LDA energies arise from the different stoichiometries of the calculations; our calculations were for $AB_2H_{0.125}$ while Hong and Fu used $AB_2H_{0.5}$. We have not pursued this topic further because it is not the main thrust of this work. The most significant difference in results between the two DFT functionals we have examined is for $ZrFe_2$. As shown in Table I, GGA predicts that g sites are more stable than e sites by 0.1 eV, while LDA predicts that the energy difference between the sites is <0.02 eV. For the other three materials listed in Table I, LDA and GGA calculations both predict the same site to be energetically preferred, although they differ by ±0.06 eV on the magnitude of the energy difference between e and g sites. All of the results reported below are from GGA-DFT calculations performed using the GGA-optimized lattice constant.

H diffusion among e and g sites in C15 AB_2 materials involves two distinct types of hops between g sites, hops from g to e sites, and the reverse e to g hop.[34,39] For each of the six materials listed above we characterized each of these hops using DFT. Once each local hopping rate is defined with the formalism above, the net self-diffusion coefficient for H in the material can be calculated.[39] If the hopping rate from e to g sites is denoted Γ_1, the reverse hopping rate by Γ_2, the hopping rate between g sites within a hexagon by Γ_3, and the hopping rate between g sites in adjacent hexagons by Γ_4, then the low concentration diffusion coefficient of H is given by[39]

$$D = \frac{a^2\Gamma_1}{32(\Gamma_2 + 3\Gamma_1)}[4\Gamma_4(1 - \Gamma_1/\Gamma_2) + 3\Gamma_2 - 5\Gamma_1 + A - B], \tag{3}$$

where

$$A = \frac{[\Gamma_2(\Gamma_3 + \Gamma_1) + 3\Gamma_3\Gamma_1](4\Gamma_4 + 5\Gamma_2) + \Gamma_2^2(2\Gamma_4 - 10\Gamma_3 - 3\Gamma_2)}{\Gamma_2(\Gamma_2 + 3\Gamma_3)}, \tag{4}$$

and

$$B = \frac{2\Gamma_4(8\Gamma_3\Gamma_4 + 5\Gamma_3^2 + 2\Gamma_2\Gamma_3 + 3\Gamma_2\Gamma_4)}{(\Gamma_2 + 3\Gamma_3)(\Gamma_3 + \Gamma_4)}, \tag{5}$$

and a is the lattice constant. The fact that diffusion coefficients can be calculated analytically in this way makes these ordered materials particularly useful for comparing theoretical models of diffusion with experimental data. Using this approach, we computed the diffusion coefficient of H in each material over a wide range of temperatures.

We first consider H diffusion in C15 $ZrCr_2$, where we can compare our results with extensive experimental data.[33,34,36] The predicted self-diffusivity of H in $ZrCr_2$ both with and without tunneling contributions is shown in Fig. 1, along with experimental data for $ZrCr_2H_{0.2}$ from Renz *et al.*[33] Harmonic TST alone is clearly incompatible with the complete set of experimental data. Including tunneling corrections, however, accurately captures the change in apparent activation energy that is observed as T is varied. Fitting our predictions to the standard Arrhenius expression, $D = \nu \exp(-E/kT)$, in the same T ranges as the experimental analysis of Majer[36] yields $E = 0.161$ eV for $T > 260$ K and 0.049 eV for $T < 170$ K. The experimental values are $E = 0.167$ and 0.046 eV, respectively.[36] An alternative analysis[33] is to fit the entire data set to $D = \nu_1 e^{-E_1/kT} + \nu_2 e^{-E_2/kT}$. Experimentally, this yields $E_1 = 0.146$–0.157 eV and $E_2 = 0.021$–0.039 eV for $ZrCr_2H_x$ with $x = 0.2$–0.5. Analyzing our data in the same way for the same range of T gives $E_1 = 0.172$ eV and $E_2 = 0.049$ eV. While the predicted activation energies are in good agreement with experiment, it is clear from Fig. 1 that the pre-exponential factor associated with diffusion is overestimated by our computational methods. We return to this point below.

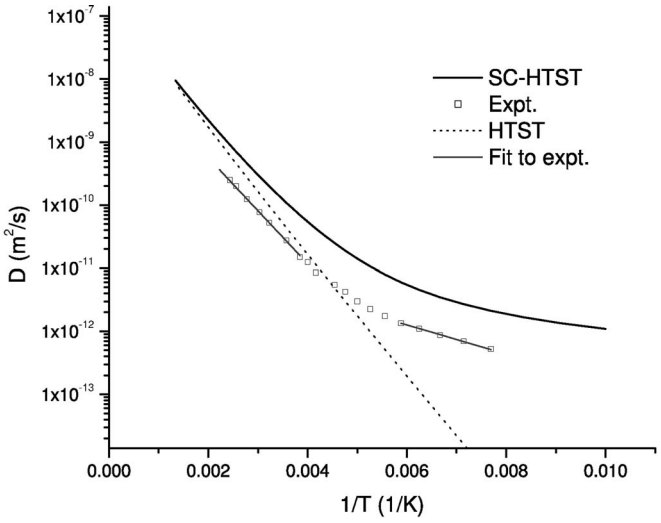

FIG. 1. The net self-diffusion rate for H in $ZrCr_2$ as predicted by harmonic transition state theory (HTST), semiclassically corrected harmonic transition state theory (SC-HTST), and as measured experimentally by Renz *et al.* (Ref. 33). The fits to the experimental data in the low and high temperature regime reported by Majer (Ref. 36) are also shown.

One convenient feature of the Fermann and Auerbach formalism is that it provides a simple estimate of the crossover temperature for an individual hopping transition, T_c, below which tunneling contributions are significant,[14] $T_c = (h\nu^{\ddagger}E_{ZP}/k)/(2\pi E_{ZP} - h\nu^{\ddagger}\ln 2)$. For H diffusion in $ZrCr_2$, the four distinct site-to-site hops yield crossover temperatures of 198, 203, 212, and 212 K. Figure 1 is consistent with these estimates; for $T < 200$ K tunneling contributions are the dominant feature of H diffusion while for $T > 200$ K the importance of tunneling decreases rapidly with increasing T.

One hallmark of tunneling processes is the existence of strong isotope effects. Once the calculations necessary in the method above have been performed for one isotope, no additional information is needed to predict isotopic effects. As an example, Fig. 2 compares the predicted diffusion coefficients of H and D in C15 $ZrCr_2$. In a purely classical setting, $D_D = D_H/\sqrt{2}$. Even in the absence of tunneling contributions, this expression is incorrect at low temperatures because the zero-point corrected activation energy defined above, E_{ZP}, is mass dependent. This can be seen from the harmonic TST results shown in Fig. 2. The isotope effect is greatly magnified when tunneling contributions are included. As can be seen in Fig. 2, below $T \sim T_c \approx 200$ K for H, the diffusion

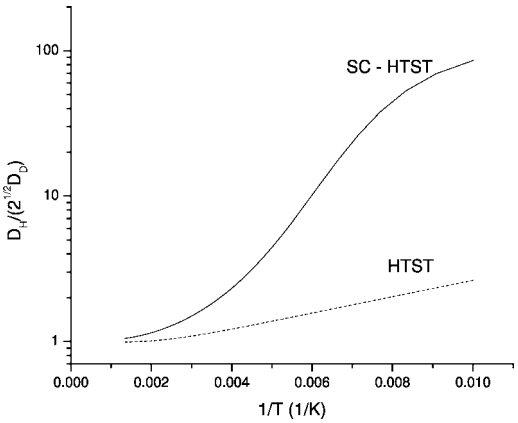

FIG. 2. The relative diffusion rates of H and D in $ZrCr_2$ as predicted by harmonic transition state theory (HTST) and semiclassically corrected harmonic transition state theory (SC-HTST).

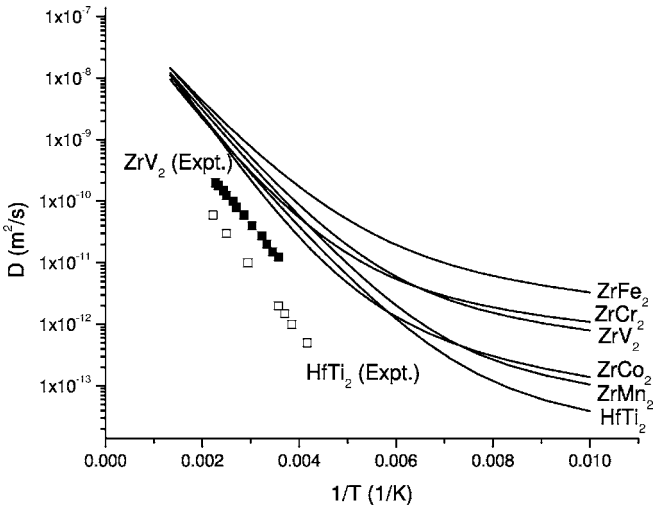

FIG. 3. The net self-diffusivities of H in six different C15 AB_2 intermetallics as predicted by semiclassically corrected harmonic transition state theory. Experimental data for ZrV_2 from Majer *et al.* (Ref. 31) and $HfTi_2$ from Eberle *et al.* (Ref. 26) are also shown.

coefficient for D is significantly lower than would be predicted by the simple scaling.

The predicted temperature dependent diffusivities for H in C15 $HfTi_2, ZrCr_2, ZrFe_2, ZrMn_2, ZrCo_2$, and ZrV_2, including tunneling contributions, are summarized in Fig. 3 and Table II. In each case, the rates of each possible hopping event were computed with the DFT-based semiclassical approach defined above and the net diffusion rate was found using the analytic expression that combines the individual rates. At room temperature and above, tunneling contributions are negligible in all six materials. At temperatures lower than 200 K, however, tunneling contributions become increasingly dominant.

The available experimental data for H diffusion in ZrV_2[31] and $HfTi_2$[26,28] is also plotted in Fig. 3. It can be seen from Fig. 3 that these data are only available in the temperature range where tunneling corrections are negligible. The effective activation energies obtained from fitting this data are compared with our theoretical predictions in Table II. As with the case of $ZrCr_2$ discussed above, our theoretical calculations accurately predict the activation energy of H diffusion.

As was also the case for $ZrCr_2$, the diffusion preexponential is substantially overestimated by our calculations for both ZrV_2 and $HfTi_2$. Part of this discrepancy presumably arises from the harmonic approximations made in our calculations. In the tunneling regime, the coupling between lattice phonons or conduction electrons and the diffusing H atom can renormalize the hopping rate.[9] As mentioned in Sec. II, the SC-HTST method we have applied here does not explicitly include these effects. Several strategies exist to deal with this shortcoming of our approach if one is interested in describing H diffusion in a complex metal alloy. First, one could use our approach to rapidly determine the most important individual hop or hops from among the set of all possible hops and then apply the computationally inten-

TABLE II. A summary of the crossover temperatures and effective activation energies for H diffusion in C15 AB_2 materials. The crossover temperature, T_c, is defined as the minimum of the crossover temperature defined in the text for hops of all types in the material. The effective activation energies are determined from fits to the Arrhenius plots in Fig. 3. For $ZrCo_2, ZrMn_2, ZrFe_2$, the high T fit used $250 < T < 500$ K and the low T fit used $130 < T < 170$ K. For $ZrCr_2, ZrV_2$, and $HfTi_2$, fits were done in same T range as the experimental data (Ref. 36) for $ZrCr_2H_{0.2}$ (Ref. 33), $ZrV_2H_{0.5}$ (Ref. 31), and $HfTi_2H_4$ (Ref. 26).

Material	T_c (K)	E_a (eV) (High T)	E_a (ev) (Low T)
$ZrCo_2$	165	0.197	0.068
$ZrMn_2$	152	0.172	0.095
$ZrFe_2$	177	0.140	0.054
$ZrCr_2$	198	0.161	0.049
		Exp.–0.167($260 < T < 445$ K)	Exp.–0.046($130 < T < 170$ K)
ZrV_2	173	0.165	0.063
		Exp.–0.179($280 < T < 445$ K)	($130 < T < 170$ K)
$HfTi_2$	77	0.177	0.107
		Exp.–0.210($220 < T < 500$ K)	($130 < T < 170$ K)

sive DFT-based approaches cited above that treat anharmonic effects and tunneling contributions in a more rigorous manner[8,9] to this reduced set of diffusion events. Second, if experimental data is available, then the individual hopping rates predicted by our approach can be effectively used as initial estimates for the refinement of models that correctly account for the variety of hops that can occur in a complex material.[27] Alternatively, if the aim is only to predict the relative diffusion rates in a series of materials then it appears that our method is sufficiently accurate with no further elaboration. As shown above, our method correctly predicts the experimental observation that H diffuses more slowly in $HfTi_2$ than in C15 ZrV_2 which in turn exhibits diffusion rates similar to C15 $ZrCr_2$. Our method predicts that diffusion in C15 $ZrFe_2$ is faster than in any of these materials, particularly at low temperatures.

IV. H DIFFUSION IN bcc CuPd

We have also used the methods described above to examine tunneling contributions to H transport in ordered bcc CuPd. CuPd alloys are of practical interest in efforts to make chemically robust membranes for hydrogen purification.[1,11,17,40–42] Several experimental studies have probed H diffusion in bcc CuPd. $Cu_{53}Pd_{47}$ was studied using Gorsky effect measurements by Lang *et al.* for temperatures ranging from 100–273 K.[43] The bcc phase was found to have diffusivity that was four orders of magnitude larger than the value in the corresponding fcc CuPd alloy at room temperature. The effective activation barrier was found to be 0.04 eV. Piper studied H diffusion in CuPd alloys using the dependence of electrical resistivity upon H concentration.[44] At $T=298$ K, the diffusivity was two orders of magnitude larger in the bcc material than in the fcc material with the same stoichiometry. The effective activation energy for diffusion reported from these experiments was 0.11 eV. Zetkin *et al.* used the method of flow determination in the dynamic regime to study diffusion of deuterium in bcc $Cu_{47}Pd_{53}$ from 600–1070 K,[45] reporting an effective activation energy of 0.10 eV. *D* diffusion is also observed to be much faster in bcc CuPd alloys than in analogous fcc CuPd alloys.[46]

Kamakoti and Sholl have previously used plane wave DFT calculations to examine H diffusion in bcc CuPd with a range of compositions around $Cu_{50}Pd_{50}$.[1,17] These calculations predict that the net diffusivity of H in these materials varies only weakly with alloy composition. As a result, we focus on ordered bcc $Cu_{50}Pd_{50}$, denoted simply CuPd below for simplicity. H resides in tetrahedral (T) sites in CuPd and can hop into adjacent sites via two inequivalent paths with different activation energies. In Ref. 17, we incorrectly stated that hops that proceed through only combinations of the pathway with the lower activation energy can lead to long range motion. In fact, hops of this type can only lead to localized motion, so it is the path with the higher activation energy that is the rate-limiting step to long-range diffusion.[1,11]

We have applied semiclassical corrected harmonic transition state theory to the rate limiting step for H diffusion in CuPd using plane wave DFT with methods analogous to those described above for C15 materials. The details of the DFT calculations are described in our earlier work.[1,17] The predicted site-to-site hopping rate, k_{TT}, is shown with and without tunneling corrections in Fig. 4. A more useful way to compare these results to the experimental data mentioned above is to define the temperature dependent activation energy for this rate by

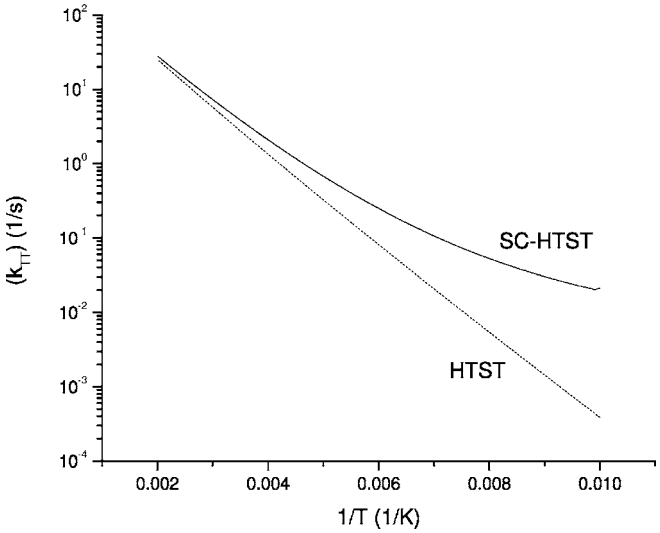

FIG. 4. The hopping rate for the rate-determining step of H diffusion in bcc CuPd as predicted by harmonic transition state theory (HTST) and semiclassically corrected harmonic transition state theory (SC-HTST).

$$E_a = \frac{\partial(\ln k_{TT})}{\partial(1/T)}. \tag{6}$$

This effective activation energy can be readily calculated by a finite difference approximation to the derivatives in Eq. (6) once k_{TT} has been calculated as a function of temperature. The resulting temperature dependent effective activation energies for H and *D* diffusion in CuPd are shown in Fig. 5.

It is clear after including the effects of tunneling that the various experiments listed above yielded different effective activation barriers because of the different ranges of temperature used in the experiments. In particular, Fig. 5 shows that a lower effective activation energy should be expected at the temperatures examined by Lang *et al.*[43] than for the room temperature measurements by Piper.[44] The barrier reported by Lang *et al.* for diffusion from 100–273 K is on the lower side of the range of values predicted theoretically in this range. The precise barrier determined for any set of experiments in the temperature range where the effective activation energy varies substantially will, of course, be dependent on the details of the temperatures used to collect data and the method of fitting the resulting data. The theoretically predicted barrier at room temperature is in very good agreement with the experimental report by Piper.[44] The theoretical prediction for *D* diffusion at high temperatures overestimates the experimental value by ~0.015 eV.

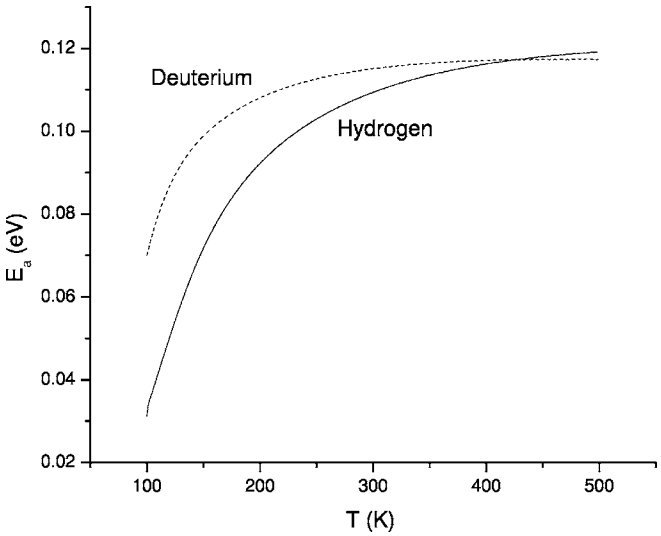

FIG. 5. The temperature dependent effective activation energy defined in Eq. (3) for the hopping rate of H and *D* in bcc CuPd.

V. CONCLUSION

In conclusion, we have shown that a combination of plane wave DFT calculations and semiclassically corrected harmonic transition state theory provides a useful description of hydrogen diffusion rates in complex metal alloys. The semiclassical formalism developed by Fermann and Auerbach uses only information that must already be determined to apply classical harmonic transition state theory, namely, the classical activation energy and the harmonic vibrational frequencies at the relevant energy minimum and transition state. This approach gives a natural means to estimate the temperature regimes where tunneling is an important contribution to H transport. Crucially, this approach is well suited to describing complex alloys in which large numbers of distinct site-to-site hops must be characterized. In some instances, for example, in studies of hydrogen permeation through metal alloy membranes at elevated temperatures, it is sufficient to know that tunneling can be neglected in modeling hydrogen transport. In cases where tunneling is found to be important under conditions of interest for a particular application, it may be appropriate to further examine specific hopping events using methods that remove some of the approximations inherent in the harmonic transition state theory approach we have used here.[8–10]

We have demonstrated the utility of the semiclassically corrected method by analyzing all possible hops within six different C15 AB_2 intermetallics. In these ordered materials, it is possible once all the local hopping rates are known to rigorously predict the net diffusion coefficient for H through these materials.[39] We also examined the rate-determining step for H diffusion in bcc CuPd. Including the effects of tunneling in this case show that the extant experimental studies are self-consistent even though there is considerable variation in the diffusion activation energies that have been observed experimentally.

Throughout this paper, we have concentrated on the diffusion of H at dilute loadings. It would be straightforward to adapt our methods to examine the impact of H loading on local hopping rates and to use this information in conjunction with Monte Carlo simulations[11,27,47–50] to explore the effects of H concentration on diffusion.

ACKNOWLEDGMENTS

This work was partially supported by the Department of Energy Coal Research Program. Preeti Kamakoti's assistance with the CuPd calculations is greatly appreciated.

*Corresponding author. FAX: 412 268 7139. Electronic address: sholl@andrew.cmu.edu

[1] P. Kamakoti, B. D. Morreale, M. V. Ciocco, B. H. Howard, R. P. Killmeyer, A. V. Cugini, and D. S. Sholl, Science **307**, 569 (2005).
[2] B. C. Hauback, H. W. Brinks, C. M. Jensen, K. Murphy, and A. J. Maeland, J. Alloys Compd. **358**, 142 (2003).
[3] J. J. Vajo, F. Mertens, C. C. Ahn, R. C. Bowman, and B. Fultz, J. Phys. Chem. B **108**, 13977 (2004).
[4] E. Lunarska and O. Chernyaeva, Mater. Sci. **40**, 399 (2004).
[5] G. Alefeld and J. Volkl, *Hydrogen in Metals I: Basic Properties* (Springer-Verlag, Berlin, 1978).
[6] Y. Fukai, *The Metal-Hydrogen System* (Springer-Verlag, Berlin, 1993).
[7] C. P. Flynn and A. M. Stoneham, Phys. Rev. B **1**, 3966 (1970).
[8] P. G. Sundell and G. Wahnström, Phys. Rev. Lett. **92**, 155901 (2004).
[9] P. G. Sundell and G. Wahnström, Phys. Rev. B **70**, 081403(R) (2004).
[10] G. Kallen and G. Wahnström, Phys. Rev. B **65**, 033406 (2001).
[11] P. Kamakoti and D. S. Sholl, Phys. Rev. B **71**, 014301 (2005).
[12] A. F. McDowell, N. L. Adolphi, and C. A. Sholl, J. Phys.: Condens. Matter **13**, 9799 (2001).
[13] J. Greeley and M. Mavrikakis, Nat. Mater. **3**, 810 (2004).
[14] J. T. Fermann and S. Auerbach, J. Chem. Phys. **112**, 6787 (2000).
[15] R. Hernandez and W. H. Miller, Chem. Phys. Lett. **214**, 129 (1993).
[16] H. Smithson, C. A. Marianetti, D. Morgan, A. Vanderven, A. Predith, and G. Ceder, Phys. Rev. B **66**, 144107 (2002).
[17] P. Kamakoti and D. S. Sholl, J. Membr. Sci. **225**, 145 (2003).
[18] J. Greeley and M. Mavrikakis, Surf. Sci. **540**, 215 (2003).
[19] D. E. Jiang and E. A. Carter, Surf. Sci. **547**, 85 (2003).
[20] S. Hong and C. L. Fu, Phys. Rev. B **66**, 094109 (2002).
[21] G. Kresse and J. Furthmüller, Comput. Mater. Sci. **6**, 15 (1996).
[22] A. Pebler and E. A. Gulbransen, Trans. Metall. Soc. AIME **239**, 1593 (1967).
[23] A. T. Pedziwiatr, R. S. Craig, W. E. Wallace and F. Pourarian, J. Solid State Chem. **46**, 336 (1983).
[24] I. Jacob, D. Davidon, and D. Shaltiel, J. Magn. Magn. Mater. **20**, 226 (1980).
[25] C. Geibel, W. Goldacker, H. Keiber, V. Ostreich, H. Rietschel, and H. Wohl, Phys. Rev. B **30**, 6363 (1984).

[26] U. Eberle, G. Majer, A. V. Skripov, and V. N. Koshanov, J. Phys.: Condens. Matter **14**, 153 (2002).
[27] B. Bhatia, X. Luo, C. A. Sholl, and D. S. Sholl, J. Phys.: Condens. Matter **16**, 8891 (2004).
[28] A. V. Skripov, J. Combet, H. Grimm, R. Hempelmann, and V. K. Kozhanov, J. Phys.: Condens. Matter **12**, 3313 (2000).
[29] G. Henkelman, B. P. Uberuaga, and H. Jónsson, J. Chem. Phys. **113**, 9901 (2000).
[30] D. E. Jiang and E. A. Carter, Phys. Rev. B **70**, 064102 (2004).
[31] G. Majer, U. Kaess, M. Stoll, R. G. Barnes, and J. Shinar, Defect Diffus. Forum **143–147** (1997).
[32] C. U. Maier and H. Kronmüller, J. Phys.: Condens. Matter **4**, 4409 (1992).
[33] W. Renz, G. Majer, A. V. Skripov, and A. Seeger, J. Phys.: Condens. Matter **6**, 6367 (1994).
[34] A. V. Skripov, M. Pionke, O. Randl, and R. Hempelmann, J. Phys.: Condens. Matter **11**, 1489 (1999).
[35] A. V. Skripov, T. J. Udovic, Q. Huang, J. C. Cook, and V. N. Kozhanov, J. Alloys Compd. **311**, 234 (2000).
[36] G. Majer, Mater. Res. Soc. Symp. Proc. **513**, 109 (1998).
[37] P. Fischer, F. Fauth, G. Bottger, A. V. Skripov, and V. N. Kozhanov, J. Alloys Compd. **282**, 184 (1999).
[38] N. F. Miron, V. I. Shcherbak, V. N. Bykov, and V. A. Levdik, Sov. Phys. Crystallogr. **16**, 266 (1971).
[39] C. A. Sholl, J. Phys.: Condens. Matter **17**, 1329 (2005).
[40] B. D. Morreale, M. V. Ciocco, B. H. Howard, R. P. Killmeyer, A. Cugini, and R. M. Enick, J. Membr. Sci. **241**, 219 (2004).
[41] F. Roa, J. D. Way, R. L. McCormick, and S. Paglieri, Chem. Eng. J. **93**, 11 (2003).
[42] F. Roa and J. D. Way, Ind. Eng. Chem. Res. **42**, 5827 (2003).
[43] J. Volkl and G. Alefield, in *Hydrogen in Metals I*, edited by G. Alefield and J. Volkl (Springer-Verlag, Berlin, 1978), Vol. 28, p. 321.
[44] J. Piper, J. Appl. Phys. **37**, 715 (1966).
[45] A. S. Zetkin, G. Kagan, E. A. N. Varakshin, and E. S. Levin, Sov. Phys. Solid State **34**, 83 (1992).
[46] A. S. Zetkin, G. Y. Kagan, and E. S. Levin, Phys. Met. Metallogr. **64**, 130 (1987).
[47] E. Salomons, J. Phys. C **21**, 5953 (1988).
[48] L. F. Perondi, R. J. Elliott, and K. Kaski, J. Phys.: Condens. Matter **38**, 7949 (1997).
[49] B. P. Uberuaga, A. F. Voter, K. K. Sieber, and D. S. Sholl, Phys. Rev. Lett. **91**, 105901 (2003).
[50] S. A. FitzGerald, R. Hannachi, D. Sethna, M. Rinkoski, K. K. Sieber, and D. S. Sholl, Phys. Rev. B **71**, 045415 (2005).